

A new insight into neutrino energy loss by electron capture of iron group nuclei in magnetars surface

Jing-Jing Liu ^{1,2} and Wei-Min Gu ¹
 syjjliu68@qzu.edu.cn; guwm@xmu.edu.cn

ABSTRACT

Based on the relativistic mean-field effective interactions theory, and Lai dong model (Lai & Shapiro 1991; Lai. 2001, 2015), we discuss the influences of superstrong magnetic fields (SMFs) on electron Fermi energy, nuclear binding energy, and single-particle level structure in magnetars surface. By using the method of Shell-Model Monte Carlo (SMMC), and the Random Phase Approximation (RPA) theory, we detailed analyze the neutrino energy loss rates (NELRs) by electron capture (EC) for iron group nuclei in SMFs. Firstly, when $B_{12} < 100$, we find that the SMFs has a slight influence on the NELR for most nuclides at relativistic low temperature (e.g., $T_9 = 0.233$), nevertheless, the NELRs increases by more than four orders of magnitude at relativistic high temperature (e.g., $T_9 = 15.53$). When $B_{12} > 100$, the NELRs decreases by more than three orders of magnitude (e.g., at $T_9 = 15.53$ for $^{52-61}\text{Fe}$, $^{55-60}\text{Co}$ and $^{56-63}\text{Ni}$). Secondly, for a certain value of magnetic field and temperature, the NELRs increases by more than four orders of magnitude when $\rho_7 \leq 10^3$, but as the density increases (i.e. when $\rho_7 > 10^3$), there are almost not influence of density on NELRs. For the density around $\rho_7 = 10^2$, there is an abrupt increase in NELRs when $B_{12} \geq 10^{3.5}$. Such jumps are an indication that the underlying shell structure has changed due to single-particle behavior by SMFs. Finally, we compare our NELRs with those of Fuller et al. (1982, 1985) (FFN), and Nabi & Klapdor-Kleingrothaus (1999) (NKK). For the case without SMFs, one finds that our rates for certain nuclei are about close to five orders magnitude lower than FFN, and NKK at relativistic low temperature (e.g., $T_9 = 1$). However, at the relativistic high temperature (e.g., $T_9 = 3$), our results are in good agreement with NKK, but about one order magnitude lower than FFN. For the case with SMFs, our NELRs for some iron group nuclei can be about five orders of magnitude higher than those of FFN, and NKK. (note B_{12} , T_9 , and ρ_7 are in unit of 10^{12}G , 10^9K , and 10^7g/cm^3 , respectively)

Subject headings: stars: magnetic fields — stars: neutron — Physical Date and Processes: nuclear reactions.

1. Introduction

In the process of core-collapse supernova explosions, neutrino processes and weak interaction (e.g. electron capture (hereafter EC) and beta decay) play pivotal roles. At the late stages of evolution, a large amount of energy from a stellar is

lost mainly through neutrinos and this process is fairly independent of the mass of star. For instance, White dwarfs and supernovae, both have cooling rates largely dominated by neutrino production. At high temperatures and densities, the EC and the accompanying neutrino energy loss rates (hereafter NELRs) are of prime importance in determining the equation of state of supernova. An accurate determination of neutrino emission rates is very necessary in order to perform a careful analysis of the final branches of stellar evolutionary tracks. The neutrino cooling rates can

¹Department of Astronomy and Institute of Theoretical Physics and Astrophysics, Xiamen University, Xiamen, Fujian 361005, China

²College of Electronic and Communication Engineering, Hainan Tropical Ocean University, Sanya, 572022, China

strongly influence on the evolutionary time scale and the configuration of iron core at the onset of the supernova explosion.

Some researches for cooling of white dwarfs, neutron stars, and magnetars need us giving a accurate estimation of some weak interaction rates and NELRs. Due to the importance of the EC and NELRs in astrophysical environments, Beaudet et al. (1967); Braaten et al. (1993); Ahmad et al. (2010); Esposito et al. (2003); Fuller et al. (1980, 1982, 1985); Itoh et al. (1996); Juodagalvis et al. (2010); Langanke et al. (2001); Langanke & Martinez-Pinedo. (1998); Liu. (2013c,d,e, 2015, 2016) have done some pioneering works on the weak interaction reactions and NELRs for some iron group nuclei. Recently, by using the proton-neutron quasi-particle random phase approximation (pn-QRPA) theory, Nabi & Sajjad (2014); Nabi & Klapdor-Kleingrothaus (1999, 2004) have detailed investigated the neutrino and anti-neutrino energy loss rates. However, their works seemed to pay no attention to the influence of superstrong magnetic fields (hereafter SMFs) on NELRs.

The neutrino processes will play a crucial role in magnetars and some neutron stars due to electron capture (EC) and beta decay. A great deal of energies and messages set free with the escape of the neutrino. Thus, the works on neutrino and the NELRs have been the hotspot and former-border issue in magnetars and some neutron stars. In order to understand the nature of the weak interaction process and NELRs in magnetars, the study of matter in SMFs is obviously an important component of magnetars in astrophysics research. Some works show that the strengths of magnetic fields at the crust of neutron stars are in the range of $10^8 - 10^{13}$ G (Baym et al. 1998; Dai et al. 1993). There has recently been growing evidence for the existence of neutron stars possessing magnetic fields with strengths that exceed the quantum critical field strength of 4.4×10^{13} G. Such evidence has been provided by new discoveries of radio pulsars having very high spin-down rates and by observations of bursting gamma-ray sources termed magnetars. In addition, some researches show that magnetars possess magnetic fields as strong as from 10^{13} G to 10^{15} G (Gao et al. 2011,?; Harding et al. 2006; Lai & Shapiro 1991; Lai. 2001, 2015; Peng et al. 2012). Although it is

not clear how strong magnetic fields in magnetars could be, some calculations indicate that fields of $10^{15} - 10^{16}$ G are not impossible. Theoretical models display that these magnetic fields might reach up to 10^{18} G, and even larger values when one considers the limit imposed by the virial theorem (Ormand et al. 1994). For such SMFs, the classical description of the trajectories of a free electron is no longer valid and quantum effect must be considered.

Previous works (Liu. 2013a,b) show that SMFs influences on electron capture rate and NELRs greatly and decreases with the increasing of the strength of magnetic field. Recent studies (Lai & Shapiro 1991; Lai. 2001, 2015) have found the magnetic field will make the Fermi surface would elongate from a spherical surface to a Landau surface along the magnetic field direction and its level is perpendicular to the magnetic field direction and strongly quantized. The properties of matter (such as atoms, molecules, and condensed matter/plasma) are dramatically changed by the superstrong magnetic fields in magnetars. Recently, due to the influence of SMFs, the electron cyclotron kinetic energy will be greater than electron-static energy in magnetars. The microscopic state number of electron momentum along the field in the interval of $P_z \sim P_z + dP_z$, is obtained via using the non-relativistic motion equation. Based on the above mentioned conditions, we detailed discuss some properties of matter of magnetar surface due to these are significantly modified by strong magnetic fields. We also analyze the influences of SMFs on NELRs from the EC reaction for some iron group nuclei.

Our work differs from previous works (Fuller et al. 1980, 1982, 1985) about the discussion of electron capture process and NELRs. Firstly, their works are based on the theory of Brink Hypothesis by FFN and overlooked the influence of SMFs on EC and NELRs. Secondly, our work also differs from the works of Nabi & Klapdor-Kleingrothaus (1999, 2004). they detailed discussed the NELRs by using the quasi-particle random phase approximation theory only in the case without SMFs. We analyze the EC process and NELRs for iron group nuclei and derive new results in SMFs according to the Shell-Model Monte Carlo (SMMC) method (Juodagalvis et al. 2010; Langanke et al. 2001). Although Juodagalvis et al. (2010); Langanke et al.

(2001) detailed discussed the EC in presupernova surrounding, but they have lost sight of the influence of SMFs on the EC process and NELR. We make detailed comparison of our results in SMFs with those of FFN, and (Nabi & Klapdor-Kleingrothaus 1999) (hereafter NKK), which are in the case without SMFs. Finally, our discussions also differs from recent works of Liu. (2013a,b), which analyzed the EC and NELRs by using the method of Brink Hypothesis. The Brink Hypothesis is a very crude approximation, which assumes that the Gamow-Teller strength distribution on excited states is the same as for the ground state, only shifted by the excitation energy of the state. By using the method of SMMC, and the RPA theory, we discuss NELRs by EC of some typical iron group nuclei basing on Lai dong model (Lai & Shapiro 1991; Lai. 2001, 2015)in SMF. Based on the relativistic mean-field effective interactions theory, we discuss the influences of SMFs on electron Fermi energy, blinding energy per nuclei, and single-particle level structure in magnetars surface. We also detailed compare our results in SMFs with those of FFN, and NKK. These NELRs of iron group nuclei may be universal, very important and helpful for the researches of thermal and magnetic evolution, particularly for study of cooling mechanisms, and numerical simulation of the neutron stars and magnetars.

The present paper is organized as follows. In the next Section, we analyze the influence of SMFs on the electron property and nuclear energy in magnetars. The studies about the EC process and NELRs in SMFs will be given in Section 3. Some numerical results and discussion are given in Section 4. And some conclusions are summarized in the last section.

2. The influence of SMFs in magnetars

2.1. How will the SMFs influence on the electron properties in magnetar surface

The properties of matter are significantly modified by strong magnetic fields, such as the states equation, electron energy, the outer crust structure and composition in neutron stars. Many works (Landau & Lifshitz. 1977; Canuto et al. 1977) detailed presented the quantum mechanics of a charged particle in SMFs. When we consider

the nonrelativistic motion of a particle (charge e_i and mass m_i) in a uniform magnetic field, which is assumed to be along the z-axis, the circular orbit radius and (angular) frequency in the process of particle gyrates are given by $r = m_i c v_{\perp} / |e_i| B$, $\omega_c = |e_i| B / m_i c$, respectively, here v_{\perp} is the velocity perpendicular to the magnetic field. The kinetic energy for electron ($m_i \rightarrow m_e$, $e_i \rightarrow -e$) of the transverse motion is quantized in Landau levels in non-relativistic quantum mechanics, and is written by

$$E_{kin} = \frac{1}{2} m_i v_{\perp}^2 \rightarrow (n_l + \frac{1}{2}) \hbar \omega_c \quad (1)$$

where $n_l = 0, 1, 2, \dots$ is Landau levels number. The cyclotron energy for a electron, which is the basic energy quantum is given by

$$E_{cyc} = \hbar \omega_c = \hbar \frac{eB}{ec} = 11.577 B_{12} \text{keV}, \quad (2)$$

where $B_{12} = B / 10^{12} \text{G}$ is the magnetic field strength in units of 10^{12} Gauss, The total electron energy, which is included the kinetic energy associated with the z-momentum (p_z) and the spin energy in non-relativistic quantum surrounding can be written as (Landau & Lifshitz. 1977; Canuto et al. 1977)

$$E_n = \nu \hbar \omega_c + \frac{p_z^2}{2m_e}, \quad (3)$$

where $\nu = n_l + (1 + \sigma_z) / 2$. $\sigma_z = -1$, $\sigma_z = \pm 1$ are the spin degeneracy for the ground Landau level ($n_l = 0$), and excited levels, respectively.

We define a critical magnetic field strength B_{cr} from the relation of $\hbar \omega_c = m_e c^2$ (i.e. $B_{cr} = m_e^2 c^3 / e \hbar = 4.414 \times 10^3 \text{G}$). The transverse motion of the electron becomes relativistic when $\hbar \omega_c \geq m_e c^2$ (i.e. $B \geq B_{cr}$) for extremely strong magnetic fields. The energy eigenstates of electron must obey the relativistic Dirac equation and is given by (Canuto et al. 1977; Johnson et al. 1949)

$$E_n = [c^2 p_z^2 + m_e^2 c^4 (1 + 2\nu \frac{B}{B_{cr}})]^{1/2}, \quad (4)$$

where the shape of the Landau wavefunction in the relativistic theory is the same as in the nonrelativistic theory due to the fact the cyclotron radius is independent of the particle mass. (Peng et al. 2012)

In SMFs the number density n_e of electrons is related to the chemical potential U_F by (Lai & Shapiro 1991; Lai. 2001, 2015; Harding et al. 2006)

$$n_e^B = \frac{1}{(2\pi\hat{\rho})^2\hbar} \sum_0^{\infty} g_{n0} \int_{-\infty}^{+\infty} f dp_z, \quad (5)$$

where $\hat{\rho} = (\hbar c/eB)^{1/2} = 2.5656 \times 10^{-10} B_{12}^{1/2}$ cm is the cyclotron radius (the characteristic size of the wave packet), and g_{n0} is the spin degeneracy of the Landau level, $g_{00} = 1$ and $g_{n0} = 2$ for $n \geq 1$, and $f = [1 + \exp((E_n - U_F)/kT)]^{-1}$ is the Fermi-Dirac distribution.

According to the relation of the usual relativistic energy and momentum from Eq.(4), the interaction energy term, which is proportional to the quantum number ν , and cannot exceed the electron chemical potential, will appears due to the electron interaction with the magnetic field. Thus the maximum number of Landau levels ν_{max} , related to the highest value of the allowed interaction energy should be satisfied with $E_n(\nu_{max}, p_z = 0) = U_F$. So we have

$$\nu_{max} = \frac{1}{2} \frac{B_{cr}}{B} \left(\frac{U_F^2}{m_e^2 c^4} - 1 \right), \quad (6)$$

However, in the general case (i.e. $0 \leq \nu \leq \nu_{max}$), when the maximum electron momentum is equaled to the Fermi momentum P_F for different Landau level value ν , the electron chemical potential from Eq.(4) can be computed as follows

$$E_n(\nu) = [c^2 p_F^2 + m_e^2 c^4 (1 + 2\nu \frac{B}{B_{cr}})]^{1/2} = U_F, \quad (7)$$

When we define a nondimensional Fermi momentum $x_e(\nu) = p_F/m_e c$, and Fermi energy $\gamma_e = U_F/m_e c^2$, the electronic density, electron energy, and pressure can be written as (Lai & Shapiro 1991)

$$n_e^B = \frac{B}{2\pi^2 B_{cr} \lambda_e^3} \sum_{\nu=0}^{\nu_{max}} g_{n0} x_e(\nu), \quad (8)$$

$$\varepsilon_e = \frac{B m_e c^2}{2\pi^2 B_{cr} \lambda_e^3} \sum_{\nu=0}^{\nu_{max}} g_{n0} (1 + 2\nu \frac{B}{B_{cr}}) \vartheta_+ \left[\frac{x_e(\nu)}{(1 + 2\nu B/B_{cr})^{1/2}} \right], \quad (9)$$

$$P_e = \frac{B m_e c^2}{2\pi^2 B_{cr} \lambda_e^3} \sum_{\nu=0}^{\nu_{max}} g_{n0} (1 + 2\nu \frac{B}{B_{cr}}) \vartheta_- \left[\frac{x_e(\nu)}{(1 + 2\nu B/B_{cr})^{1/2}} \right], \quad (10)$$

where $\vartheta_{\pm}(x) = \frac{1}{2} x \sqrt{1+x^2} \pm \frac{1}{2} \ln(x + \sqrt{1+x^2})$, $\lambda_e = \hbar/m_e c$ is the electron Compton wavelength.

2.2. How will the SMFs influence on the energy of nucleus in magnetar surface

The matter in the outer crust of a cold ($T = 0$ K) magnetar consists of a Coulomb lattice of completely ionized atoms and a uniform Fermi gas of relativistic electrons. The Gibbs free energy per baryon $g(A, Z, P)$ at a constant pressure and zero temperature can be given by

$$g(A, Z, P) = \frac{E(A, Z, P) + PV}{A} = \varepsilon + \frac{P}{n}, \quad (11)$$

where ε is the corresponding energy per nucleon, $n = A/V$ is the baryon density in a cell, and V is the volume occupied by a unit cell of the Coulomb lattice. The energy per nucleon ε , which consists of three different contributions from nuclear, electronic, and lattice is given by

$$\varepsilon = \varepsilon_n(A, Z) + \varepsilon_e(A, Z, P) + \varepsilon_l(A, Z, n), \quad (12)$$

where the nuclear contribution to the total energy per nucleon is simple and independent of the density and is written by

$$\varepsilon_n(A, Z) = \frac{M(A, Z)}{A} = \frac{1}{A} [z m_p + (A-Z) m_n - \varepsilon_{bind}(A, Z)], \quad (13)$$

where $M(A, z)$ is the nuclear mass, $\varepsilon_{bind}(A, Z)$ is the corresponding binding energy, and m_n and m_p are neutron and proton masses, respectively.

Based on the relativistic mean-field effective interactions theory of NL3 (Lalazissis et al. 1997) and DD-ME2 (Lalazissis et al. 2005), Peña Arteaga et al. (2011) detailed discussed the influence of SMFs on the nuclear binding energies. Based on a covariant density functional, an effective Lagrangian with nucleons and mesons is given by simple and independent of the density and is written by (Gambhir et al. 1990; Vretenar et al. 2005)

$$L = L_N + L_m + L_{int} + L_{BO} + L_{BM}, \quad (14)$$

where L_N , L_m , and L_{int} are the Lagrangian of the free nucleon, the free meson fields and the electromagnetic field generated by the proton, and

the Lagrangian describing the interactions, respectively. These Lagrangian are represented by

$$L_N = \bar{\psi}(i\gamma^\mu\partial_\mu - m_{nu})\psi, \quad (15)$$

$$L_m = \frac{1}{2}\partial_\mu\sigma\partial^\mu\sigma - \frac{1}{2}m_\sigma\sigma^2 - \frac{1}{4}\Omega_{\mu\nu}\Omega^{\mu\nu} + \frac{1}{2}m_\omega^2\omega_\mu\omega^\mu - \frac{1}{4}\vec{R}_{\mu\nu}\vec{R}^{\mu\nu} + \frac{1}{2}m_\rho^2\vec{\rho}_\mu\vec{\rho}^\mu - \frac{1}{4}F_{\mu\nu}F^{\mu\nu} - U(\sigma), \quad (16)$$

$$L_{int} = -g_\sigma\bar{\psi}\sigma\psi - g_\omega\bar{\psi}\gamma^\mu\omega_\mu\sigma\psi - g_\rho\bar{\psi}\gamma^\mu\vec{\tau}\vec{\rho}^\mu\psi - e\bar{\psi}\gamma^\mu A_\mu\psi, \quad (17)$$

where ψ is the Dirac spinor. m_{nu} , and $m_\sigma, m_\omega, m_\rho$, are the nucleon and meson masses, respectively. $U(\sigma) = (g_2/3)\sigma^3 + (g_3/4)\sigma^4$ is the standard form for the nonlinear coupling of the σ meson field. $g_\sigma, g_\omega, g_\rho, e$ are the coupling constants for the σ, ω, ρ , and the electric charge for photon, respectively.

The coupling of the proton orbital motion with the external magnetic field, and the coupling of protons and neutrons intrinsic dipole magnetic moments with the external magnetic field can be respective expressed as (Bjorken & Drell. 1964)

$$L_{BO} = e\bar{\psi}\gamma^\mu A_\mu^{(ext)}\psi, \quad (18)$$

$$L_{BM} = -\bar{\psi}\chi_{\tau_3}^{(ext)}\psi, \quad (19)$$

where $\chi_{\tau_3}^{(ext)} = \kappa_{\tau_3}\mu_N\frac{1}{2}\sigma_{\mu\nu}F^{(ext)\mu\nu}$, $F^{(ext)\mu\nu}$ is the external field strength tensor. $\sigma_{\mu\nu} = \frac{i}{2}[\gamma^\mu, \gamma^\nu]$, $\mu_N = e\hbar/2m$ is the nuclear magneton, $\kappa_n = g_n/2$, $\kappa_p = g_p/2 - 1$ (here $g_n = -3.8263$, $g_p = 5.5856$) are the intrinsic magnetic moments of protons and neutrons, respectively.

The electronic contribution is modeled as a degenerate free Fermi gas and is given by

$$\varepsilon_e(A, z, P) = \frac{1}{n\pi^2} \int_0^{p_F} p^2 \sqrt{p^2 + m_e^2} c^4 dp = \frac{m_e^4 c^8}{8n\pi^2} [x_e(\nu)\gamma_e(x_e^2(\nu) + \gamma_e^2) - \ln(x_e(\nu) + \gamma_e)] \quad (20)$$

The lattice energy per baryon $\varepsilon_l(A, Z, n)$ may be written as (Shapiro & Teukolsky 1983)

$$\varepsilon_l(A, Z, n) = -1.81962 \frac{(ze)^2}{a} = -C_{bcc} \frac{z^2}{A^{4/3}} p_F, \quad (21)$$

where $C_{bcc} = 3.40665 \times 10^{-3}$, and a is the lattice constant. Similar calculations such as fcc-centered cubic or simple cubic ones can be carried out evaluating different lattice configurations.

3. The NELRs due to EC in magnetars

3.1. The SMMC method and Gamow-Teller response functions

The Gamow-Teller (GT) properties of nuclei in the medium mass region of the periodic table are crucial determinants in the process of electron capture. Some works (Fassio-Canuto, L. 1969; Canuto et al. 1977) demonstrated that the GT transition matrix elements for electron capture and beta decay don't depend on the magnetic fields. Thus we will neglect the effect of SMFs on the GT properties of nuclei in this paper. The SMMC method is based on a statistical formulation of the nuclear many-body problem. We use the shell model Monte Carlo (SMMC) approach to find the GT strength distributions. SMMC has the added advantage that it treats nuclear temperature exactly. Based on a statistical formulation of the nuclear many-body problem, in the finite-temperature version of this approach, an observable is calculated as the canonical expectation value of a corresponding operator \hat{A} by the SMMC method at a given temperature T , and is written by (Koonin et al. 1992; Ormand et al. 1994; Alhassid et al. 1994; Johnson et al. 1993)

$$\hat{A} = \frac{\text{Tr}_A[\hat{A}e^{-\beta\hat{H}}]}{\text{Tr}_A[e^{-\beta\hat{H}}]}, \quad (22)$$

The problem of shell model Hamiltonian \hat{H} have been detailed investigated by Alhassid et al. (1994). When some many-body Hamiltonian \hat{H} is given, a tractable expression for the imaginary time evolution operator is written by

$$\hat{U} = \exp^{-\beta\hat{H}}, \quad (23)$$

where $\beta = 1/T_N$, T_N is the nuclear temperature in units of Mev. $\text{Tr}_A \hat{U}$ is the canonical partition function for A nucleons. In terms of a spectral expansion, the total strength of a transition operator \hat{A} is then given by the following expectation value:

$$B(A) \equiv \langle \hat{A}^\dagger \hat{A} \rangle = \frac{\sum_{i,f} e^{-\beta E_i} |\langle f | \hat{A} | i \rangle|^2}{\sum_i e^{-\beta E_i}}, \quad (24)$$

here $|i\rangle, |f\rangle$ are the many-body states of the initial (final) nucleus with energy E_i, E_f , respectively.

The SMMC method is used to calculate the response function $R_A(\tau)$ of an operator \hat{A} at an imaginary-time τ . By using a spectral distribution of initial and final states $|i\rangle$ and $|f\rangle$ with energies E_i and E_f . $R_A(\tau)$ is given by (Dean et al. 1998; Langanke et al. 2001; Langanke & Martinez-Pinedo. 1998)

$$\begin{aligned} R_A(\tau) &\equiv \langle \hat{A}^\dagger(\tau)\hat{A}(0) \rangle = \frac{\text{Tr}_A[e^{-(\beta-\tau)\hat{H}}\hat{A}^\dagger e^{-\tau\hat{H}}\hat{A}]}{\text{Tr}_A[e^{-\beta\hat{H}}]} \\ &= \frac{\sum_{if}(2J_i+1)e^{-\beta E_i}e^{-\tau(E_f-E_i)}|\langle f|\hat{A}|i\rangle|^2}{\sum_i(2J_i+1)e^{-\beta E_i}} \end{aligned} \quad (25)$$

Note that the total strength for the operator is given by $R(\tau = 0)$. S_{GT+} is the total amount of GT strength available for an initial state is given by summing over a complete set of final states in GT transition matrix elements $|M_{GT}|_{if}^2$. The strength distribution is given by (Dean et al. 1998)

$$\begin{aligned} S_{GT+}(E) &= \frac{\sum_{if}\delta(E-E_f+E_i)(2J_i+1)e^{-\beta E_i}|\langle f|\hat{A}|i\rangle|^2}{\sum_i(2J_i+1)e^{-\beta E_i}} \\ &= S_A(E), \end{aligned} \quad (26)$$

which is related to $R_A(\tau)$ by a Laplace Transform, $R_A(\tau) = \int_{-\infty}^{\infty} S_A(E)e^{-\tau E}dE$. Note that here E is the energy transfer within the parent nucleus, and that the strength distribution $S_{GT+}(E)$ has units of Mev^{-1} .

3.2. The NELRs and EC process in the case without SMFs

Based on the RPA theory with a global parameterization of the single particle numbers, the stellar electron capture rates which is related to the electron capture cross-section for the k th nucleus (Z, A) in thermal equilibrium at temperature T is given by a sum over the initial parent states i and the final daughter states f in the case without SMFs (Dean et al. 1998; Langanke et al. 2001; Langanke & Martinez-Pinedo. 1998)

$$\lambda_{ec}^0 = \frac{1}{\pi^2\hbar^3} \sum_{if} \int_{\varepsilon_0}^{\infty} p_e^2 \sigma_{ec}(\varepsilon_e, \varepsilon_i, \varepsilon_f) f(\varepsilon_e, U_F, T) d\varepsilon_e \quad (27)$$

where $\varepsilon_0 = \max(Q_{if}, m_e c^2)$. $p_e = \sqrt{\varepsilon_e^2 - m_e^2 c^4}$ is the momenta of the incoming electron, and ε_e is the total rest mass and kinetic energies of the incoming electron, U_F is the electron chemical po-

tential, T is the electron temperature. The electron Fermi-Dirac distribution is defined as

$$f = f(\varepsilon_e, U_F, T) = [1 + \exp(\frac{\varepsilon_e - U_F}{kT})]^{-1} \quad (28)$$

Due to the energy conservation, the electron, proton and neutron energies are related to the neutrino energy, and Q -value for the capture reaction (Cooperstein et al. 1984; Juodagalvis et al. 2010)

$$Q_{i,f} = \varepsilon_e - \varepsilon_\nu = \varepsilon_n - \varepsilon_p = \varepsilon_f^n - \varepsilon_i^p \quad (29)$$

and we have

$$\varepsilon_f^n - \varepsilon_i^p = \varepsilon_{if}^* + \hat{\mu} + \Delta_{np} \quad (30)$$

where $\hat{\mu} = \mu_n - \mu_p$, the difference between neutron and proton chemical potentials in the nucleus and $\Delta_{np} = M_n c^2 - M_p c^2 = 1.293 \text{ Mev}$, the neutron and the proton mass difference. $Q_{00} = M_f c^2 - M_i c^2 = \hat{\mu} + \Delta_{np}$, with M_i and M_f being the masses of the parent nucleus and the daughter nucleus respectively; ε_{if}^* corresponds to the excitation energies in the daughter nucleus at the states of the zero temperature.

The electron chemical potential is found by inverting the expression for the lepton number density (Aufderheide et al. 1990; Fuller et al. 1980, 1982, 1985)

$$n_e = \frac{8\pi}{(2\pi)^3} \int_0^{\infty} p_e^2 (f_{-e} - f_{+e}) dp_e \quad (31)$$

where $f_{-e} = [1 + \exp((\varepsilon_e - U_F)/kT)]^{-1}$ and $f_{+e} = [1 + \exp((\varepsilon_e + U_F)/kT)]^{-1}$ are the electron and positron distribution functions respectively, k is the Boltzmann constant.

According to the Shell-Model Monte Carlo method, which discussed the GT strength distributions, the total cross section by EC is given by (Dean et al. 1998; Juodagalvis et al. 2010)

$$\begin{aligned} \sigma_{ec} &= \sigma_{ec}(E_e) = \sum_{if} \frac{(2J_i+1) \exp(-\beta E_i)}{Z_A} \sigma_{fi}(E_e) \\ &= 6g_{wk}^2 \int d\xi (E_e - \xi)^2 \frac{G_A^2}{12\pi} S_{GT+}(\xi) F(Z, \varepsilon_e) \end{aligned} \quad (32)$$

where $\beta = 1/T_N$ is the inverse temperature, T_N is the nuclear temperature and in unit of Mev , and $E_e = \varepsilon_e$ is the electron energy. S_{GT+} is the

GT strength distribution, which is as a function of the transition energy ξ . The $g_{wk} = 1.1661 \times 10^{-5} \text{Gev}^{-2}$ is the weak coupling constant and G_A is the axial vector form-factor which at zero momentum is $G_A = 1.25$. $F(Z, \varepsilon_e)$ is the Coulomb wave correction which is the ratio of the square of the electron wave function distorted by the coulomb scattering potential to the square of wave function of the free electron.

By folding the total cross section with the flux of a degenerate relativistic electron gas, the NELRs due to EC in the case without SMFs is given by

$$\lambda_{\text{NEL}}^0 = \frac{\ln 2}{6163} \int_0^\infty d\xi S_{GT} \frac{c^3}{(m_e c^2)^5} \int_{p_0}^\infty dp_e p_e^2 (-\xi + \varepsilon_e)^3 F(Z, \varepsilon_e) f(\varepsilon_e, U_F, T) \quad (\text{s}^{-1}) \quad (33)$$

where the ξ is the transition energy of the nucleus, and $f(\varepsilon_n, U_F, T)$ is the electron distribution function. The p_0 is defined as

$$p_0 = \begin{cases} \sqrt{Q_{if}^2 - m_e^2 c^4} & (Q_{if} < -m_e c^2) \\ 0 & (\text{otherwise}). \end{cases} \quad (34)$$

3.3. The NELRs due to EC process in the case with SMFs

The NELRs due to EC in an SMFs from one of the initial states to all possible final states is given by

$$\lambda_{\text{NEL}}^{\text{B}} = \frac{\ln 2}{6163} \int_0^\infty d\xi S_{GT} \frac{c^3}{(m_e c^2)^5} f_{if}^{\text{B}}. \quad (35)$$

According to the method of SMMC and RPA theory, we can find the phase space factor f_{if}^{B} in SMFs, and it is defined as

$$f_{if}^{\text{B}} = \frac{c^3}{(m_e c^2)^5} \frac{b}{2} \sum_0^\infty \theta_n = \frac{c^3}{(m_e c^2)^5} \frac{b}{2} \sum_0^\infty g_{n0} \int_{p_0}^\infty dp_e p_e^2 (-\xi + \varepsilon_n)^3 F(Z, \varepsilon_n) f, \quad (36)$$

where $b = B/B_{cr}$, and the ε_n is the total rest mass and kinetic energies; $F(Z, \varepsilon_n)$ is the Coulomb wave correction which is the ratio of the square of the electron wave function distorted by the coulomb scattering potential to the square of wave function of the free electron. We assume that a SMFs

will have no effect on $F(Z, \varepsilon_n)$, which is valid only under the condition that the electron wave-functions are locally approximated by the plane-wave functions. (Dai et al. 1993) The condition requires that the Fermi wavelength $\lambda_F \sim \hbar/P_F$ (P_F is the Fermi momentum without a magnetic field) be smaller than the radius $\sqrt{2}\zeta$ (where $\zeta = \lambda_e/b$) of the cylinder which corresponds to the lowest Landau level (Baym et al. 1998).

The p_0 is defined as

$$p_0 = \begin{cases} \sqrt{Q_{if}^2 - \Theta}, & (Q_{if} < \Theta^{1/2}) \\ 0 & (\text{otherwise}), \end{cases} \quad (37)$$

where $\Theta = m_e^2 c^4 (1 + 2\nu B/B_{cr}) = m_e^2 c^4 (1 + 2\nu b)$.

4. Some numerical results and discussion

An SMFs can significantly affect the cooling properties and thermal structure of a neutron star crust. In general, the thermal insulation can be decreased by the magnetic field due to Landau quantization of electron motion. However, the thermal insulation of the envelope may be increased by the tangential magnetic field, which parallel to the stellar surface due to the fact that the Larmor rotation of the electron significantly reduces the transverse thermal conductivity. An SMFs also strongly affects the cooling curve of a neutron star and magnetar. This is because for a given core temperature, the time evolution largely depends on neutrino emission from the surface and core of a neutron star and magnetar.

Figures 1-4 display the NELRs of some iron group nuclei as a function of the magnetic field B_{12} at relatively low, and medium density (i.e. $\rho_7 = 5.86, 14.5$) and some typical temperature surrounding (i.e. $T_9 = 0.233, 15.53$). One finds that when $B_{12} < 100$ and at relatively low temperature (e.g. $T_9 = 0.233$) the magnetic field has a slight effect on the NELRs for most nuclides from Figure 1 and 3. But the NELR of most nuclides are influenced greatly at relatively high temperature (e.g. $T_9 = 15.53$). For example, for most iron group nuclei (e.g. $^{52-61}\text{Fe}$, $^{55-60}\text{Co}$ and $^{56-63}\text{Ni}$), the NELRs increases by more than four orders of magnitude at $T_9 = 15.53$ when $B_{12} < 100$. However, the NEL rates decrease by more than three orders of magnitude when $B_{12} > 100$ in Figure 1, but $B_{12} > 200$ in Figure 2.

From Figure 1 to 4, we detailed discuss the NELRs due to EC process according to SMMC method, especially for the contribution for EC due to the GT transition base on RPA theory. One finds that the influences of SMFs on NELR are significant. It is due to the fact that we have more available phase space for electron in the higher the magnetic field at a given density. On the other hand, the electron is very relativistic in the crust of magnetar, where the matter density is higher and magnetic field strength may greatly exceed the surface value. The mean Fermi energy of an electron will exceed its rest-mass energy at sufficiently high density. The electron also is very relativistic when the cyclotron energy of an electron also higher than its rest-mass energy at sufficiently high magnetic field. The electron capture will rapid occur when the electron energy becomes larger than the difference between the neutron and proton rest-mass energy (about 1.3MeV). This EC process will destroy electrons and emit massive neutrino, thereby changing the composition of matter and softening the state equation of magnetar surface.

The cross sections (hereafter ECCS) are very important parameter in electron capture process. We find the influence of SMFs on ECCS at different temperature is very significant for some nuclides due to the difference of Q-value. Given the significant energy dependence of cross sections for a process like electron capture on nuclei, it is clear that in some cases the rates will be increased at the same temperature and density as the magnetic field increases. With increasing of electron energy, the ECCS increases according to our investigations. The higher the temperature, the faster the changes of ECCS becomes. It is because that the higher the temperature, the larger the electron energy becomes. Thus even more electrons will join in the EC process due to their energy is greater than the Q-values. Furthermore, the GT transition may be dominated at high temperature surroundings. On the other hand, the trigger mechanism of electron capture process requires a minimum electron energy given by the mass splitting between parent and daughter (i.e. Q_{if}). The EC threshold energy is lowered by the internal excitation energy at finite temperature. The GT strength for even-even parent nuclei centered at daughter excitation energies of order of

2MeV at low temperatures. Therefore, the ECCS for these parent nuclei increase drastically within the first couple of MeV of electron energies above threshold, which will reflecting the GT distribution. But the GT distribution for odd-A nuclei will peak at noticeably higher daughter excitation energies at low temperatures. So the ECCS are shifted to higher electron energies for odd-A nuclei in comparison to even-even parent nuclei by about 3 MeV.

However, from figures 1-4, one finds that a systematic decrease in neutrino energy loss rate when $B_{12} > 100$. We know that the Landau energy level spacing will become a very small fraction for the Fermi energy when $\nu_{max} \gg 1$. The continuous integral may take in lieu of the discrete sum over all Landau level. The thermodynamic relation will reduce to the case of non-magnetic fields. We have $\nu_{max} \rightarrow U_e/\hbar\omega_c$ when the electron gas is of mildly relativistic state. For relativistic electron gas, the $\nu_{max} \geq 100/B_{12}$ when the $U_e \geq 1\text{MeV}$. Therefore, as magnetic field strength increases (i.e. when $B_{12} \geq 10 \sim 100$), the ν_{max} will tend to the order of unity (or zero), and the field will be termed strongly quantizing. On the other hand, The structure at the outer crust of magnetars is fundamentally determined by the energies of isolated nuclei, the kinetic energy of electrons and the lattice energy. Thus its composition is strongly depends on the binding energy per particle of stable and unstable nuclei in the outer crust of magnetar below the neutron drip density. Based on the relativistic mean-field effective interactions NL3 (Lalazissis et al. 1997) and DD-ME2 (Lalazissis et al. 2005), the influences of SMFs on the binding energy of nuclei have been investigated following the works of Peña Arteaga et al. (2011) and Basilico et al. (2015). We find that the binding energy per particle will have a mean parabolic increasing trend with increasing of the magnetic field. For example, the binding energy increase by 0.311MeV, 0.632MeV, 0.445MeV for ^{56}Fe , ^{78}Ni , ^{56}Co , respectively when the magnetic field strength from 10^{17}G to 10^{18}G . Due to increase of nuclear binding energy, the nuclear will be more stable. This is equivalent to significantly raise the threshold energy of EC reaction. Thus, the NELRs and EC rates will decreased in SMFs. Meanwhile, as the magnetic field strength increases, the electron Fermi energy will decrease

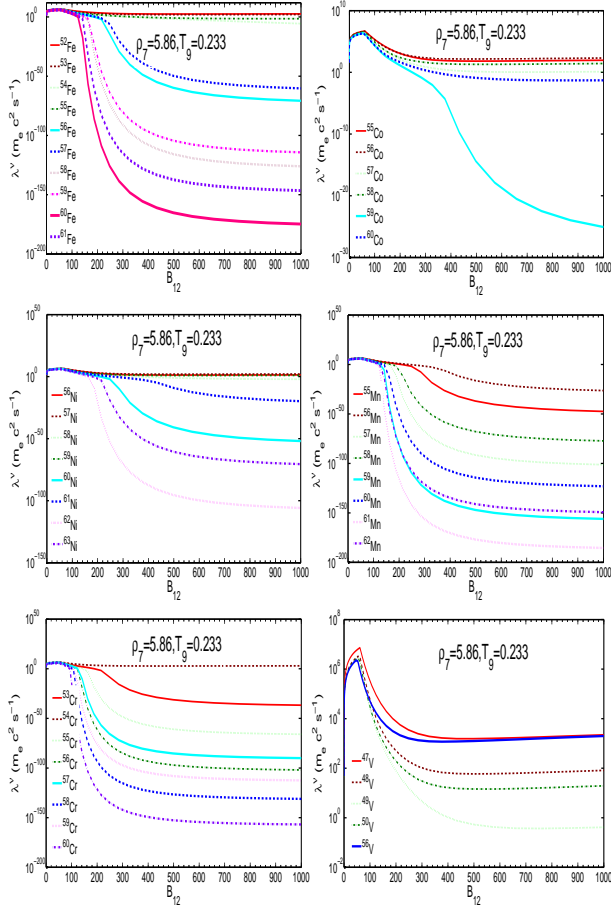


Fig. 1.— The NELRs for some typical iron group nuclei as a function of B_{12} at $\rho_7 = 5.86, T_g = 0.233$

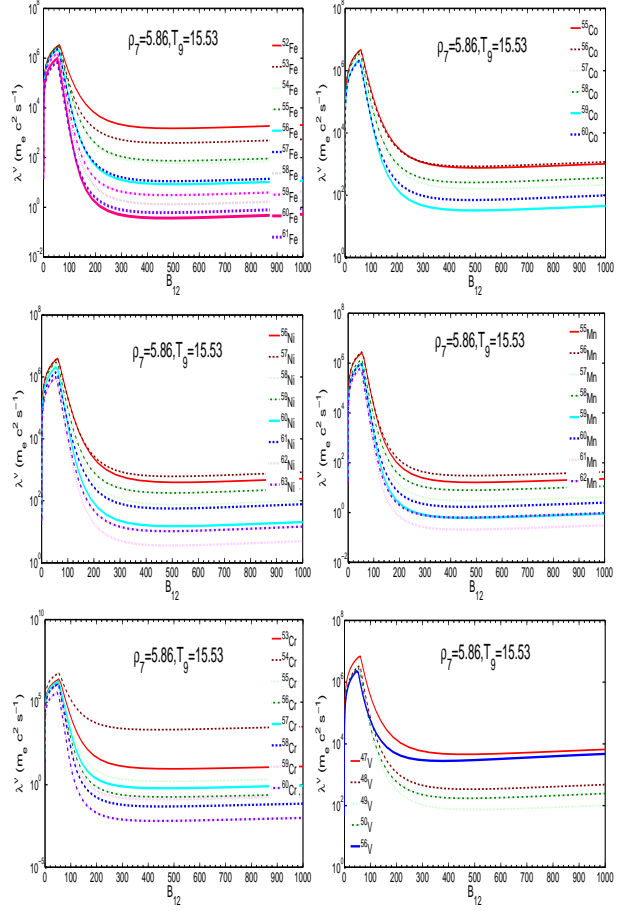


Fig. 2.— The NELRs for some typical iron group nuclei as a function of B_{12} at $\rho_7 = 5.86, T_g = 15.53$

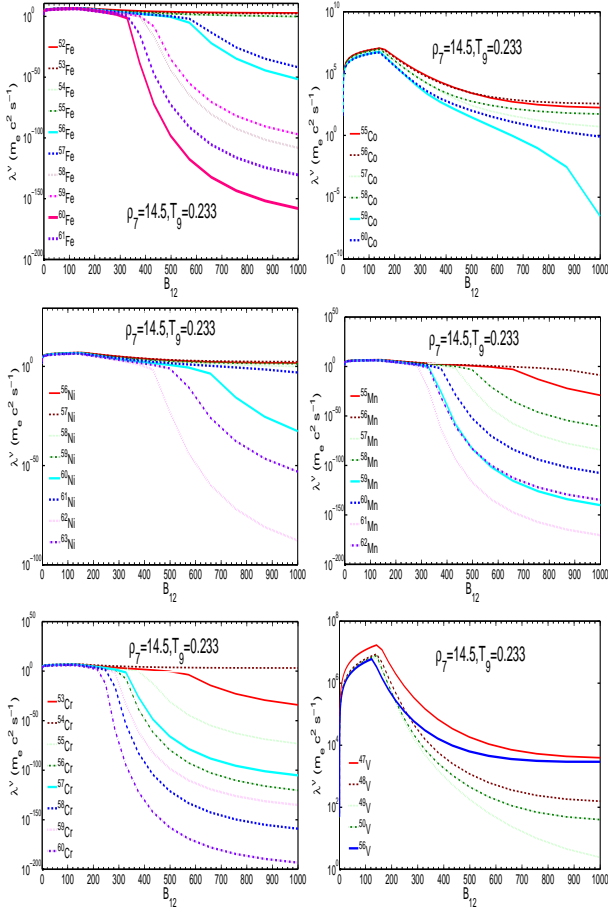


Fig. 3.— The NELRs for some typical iron group nuclei as a function of B_{12} at $\rho_7 = 14.5$, $T_9 = 0.233$

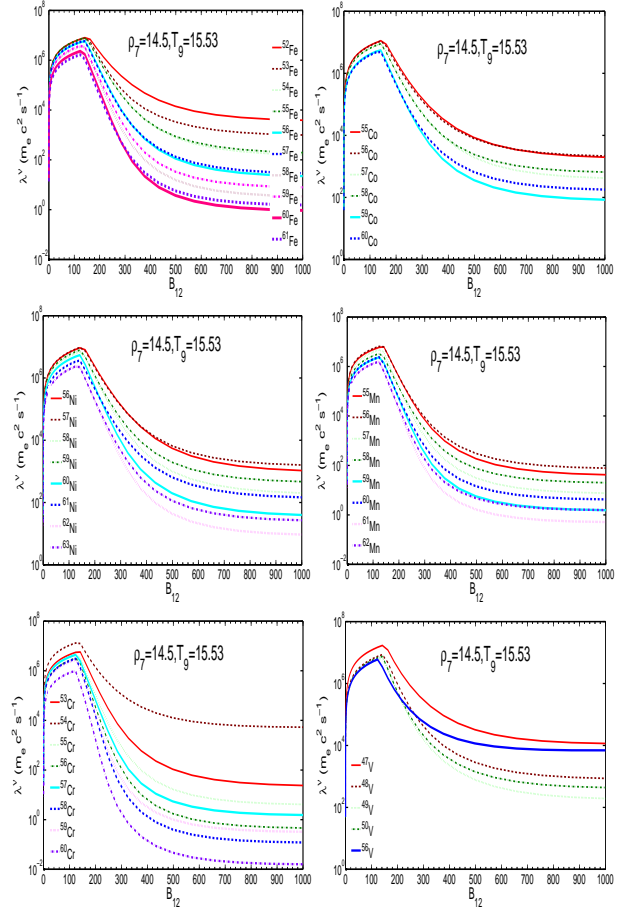


Fig. 4.— The NELRs for some typical iron group nuclei as a function of B_{12} at $\rho_7 = 14.5$, $T_9 = 15.53$

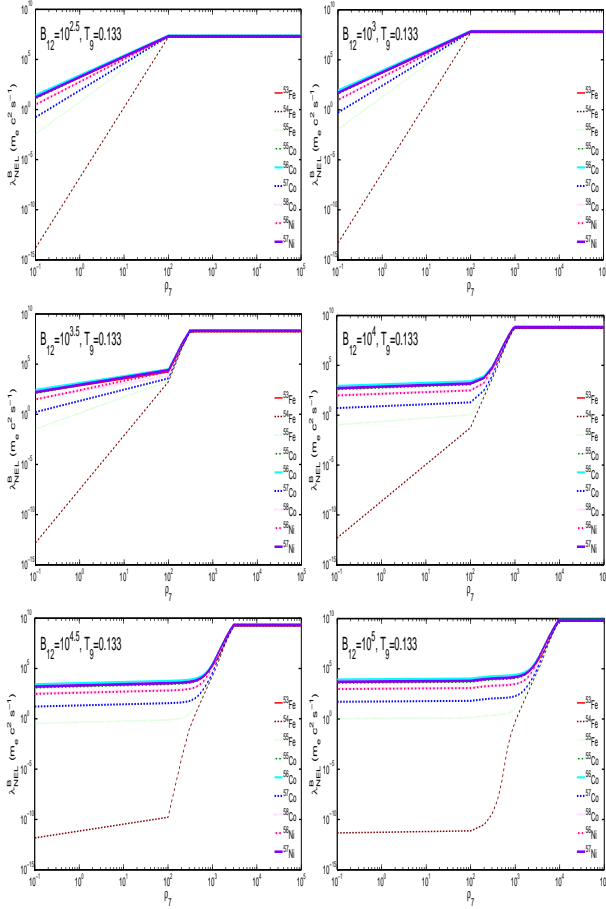


Fig. 5.— The NELRs for some typical iron group nuclei as a function of ρ_7 at $B_{12} = 10^{2.5}, 10^3, 10^{3.5}, 10^4, 10^{4.5}, 10^5$, and $T_9 = 0.133$

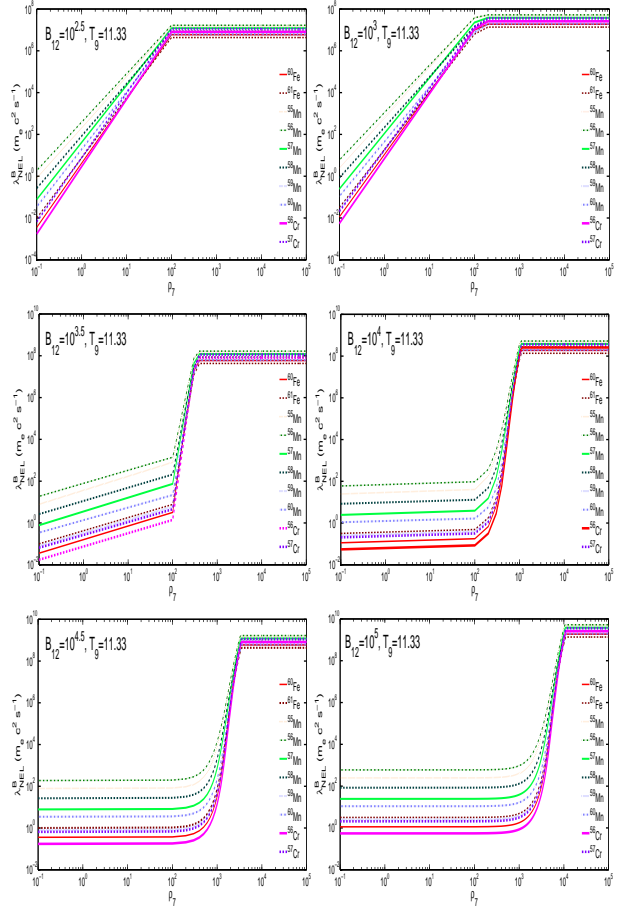


Fig. 6.— The NELRs for some typical iron group nuclei as a function of ρ_7 at $B_{12} = 10^{2.5}, 10^3, 10^{3.5}, 10^4, 10^{4.5}, 10^5$, and $T_9 = 11.33$

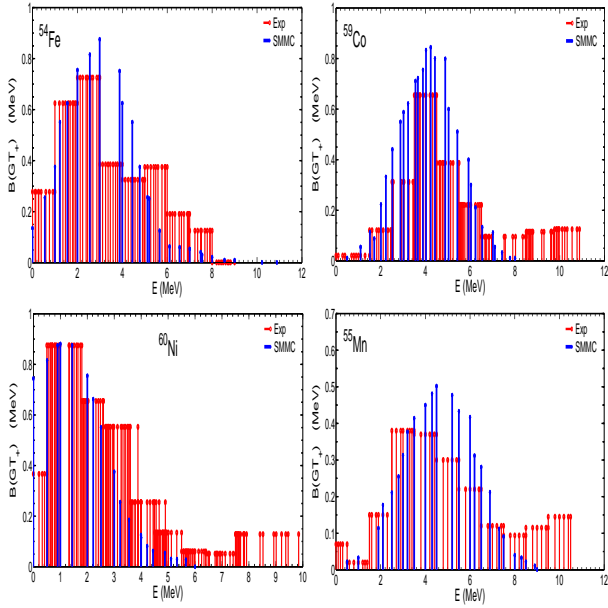


Fig. 7.— The comparison of calculated $B(GT_+)$ strength distribution against experiment(Alford et al. 1993; Williams et al. 1995; El-Kateb et al. 1994; Rapaport et al. 1984) for some typical iron group nuclei as a function of excitation energy in the corresponding daughter nuclei at temperature $T = 0.8\text{MeV}$

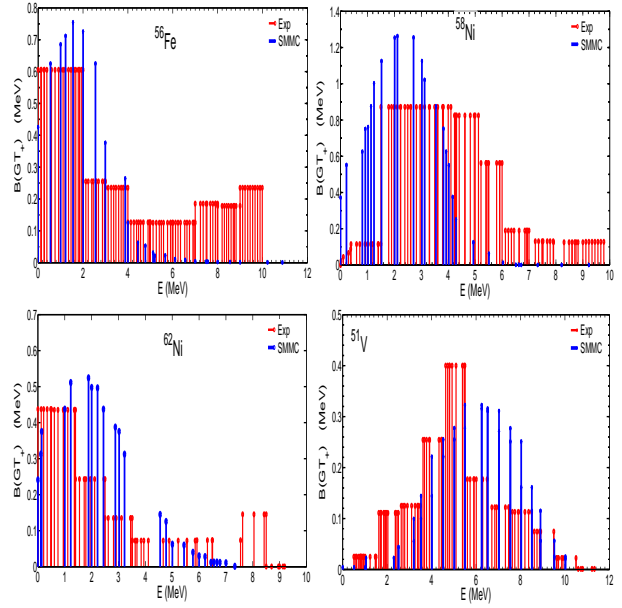


Fig. 8.— The comparison of calculated $B(GT_+)$ strength distribution against experiment(Alford et al. 1993; Williams et al. 1995; El-Kateb et al. 1994; Rapaport et al. 1984) for some typical iron group nuclei as a function of excitation energy in the corresponding daughter nuclei at temperature $T = 0.8\text{MeV}$

greatly due to interaction between the electrons and SMFs. This actually discourages the EC reaction. So the the NELRs and EC rates decrease.

The magnetic field strongly effects on the electron phase space, Only axial symmetry is preserved, and breaks spherical symmetry for the Dirac and Klein-Gordon equations (Peña Arteaga et al. 2011). For a certain value of magnetic field, Figures 5-6 present the NELRs of some typical iron group nuclei versus the density ρ_7 at temperature of $T_9 = 0.133, 11.33$. One finds that the NELRs increase greatly and even exceed by four orders of magnitude for a certain value of magnetic field and temperature. With increasing of the density, there are almost not influence of density on NELRs. On the other hand, for the density around $\rho_7 = 10^2$, there is an abrupt increase in NELRs when $10^{3.5} \leq B_{12} \leq 10^5$. Such jumps are an indication that the underlying shell structure has changed in a fundamental way. These jumps in nuclear properties can be traced to the single-particle behavior due to SMFs. As the magnetic field increases, a particle will remove from a level going upwards and bring to a level going downward with increasing spin. Furthermore, the nucleus becomes spin-polarized due to these two levels have opposite angular momentum along the symmetry axis.

The SMFs influences on the single-particle structure of nuclei for protons and neutrons. Firstly, the interaction between the magnetic field and the neutron (proton) magnetic dipole moment will cause nucleon paramagnetism. Secondly, the coupling of the orbital motion of protons with the magnetic field will also cause proton orbital magnetism. Due to the interaction between the nucleus and SMFs, all degeneracies in the single-particle spectrum may be removed, and the formerly degenerate levels with opposing signs of angular momentum projection will also tends to break (as a example, for ^{56}Fe , the detailed discussions can be seen from Figs. 3 and 5 of Ref.(Peña Arteaga et al. 2011)). Such single-particle energy splitting will produce a reduction of the neutron and proton pairing gaps with increasing magnetic fields and, eventually, their disappearance

According to the discussion of the influences from the single-particle level by SMFs, one finds that the Kramer's degeneracy in angular momen-

tum projection of proton levels is removed by the orbital magnetism associated with proton ballistic dynamics, which can bring those aligned with the magnetic field down in energy. On the other hand, the paramagnetic response (Pauli magnetism) also removes the angular momentum projection degeneracy for both protons and neutrons.

Synthesizes the above analysis, one can concludes that the last occupied single-particle levels(e.g., for ^{56}Fe)for neutron, including the influence of the proton orbital coupling and the anomalous magnetic moments coupling, decreases as the magnetic field strength increases. However, the last occupied single-particle levels for proton will increase. As is known to all, the EC is actually the process that protons will turn into neutrons and discharge a neutrino when a nuclei capture an electron. Thereby, to a certain extent, these influences of SMFs on single-particle level for proton and neutron states, ultimately make the EC reaction become more active and increase the NELRs.

The SMFs may not directly influence on the lattice energy. Nevertheless, some indirect influence on the lattice configuration will be caused by Coulomb screening. We find energetically favorable to arrange the ionized nuclei in a Coulomb lattice in the typical density range of the magnetar surface(i.e. $10^4\text{g/cm}^3 \sim 4 \times 10^{11}\text{g/cm}^3$). In relativistic lower range of density, the electron energy and the Coulomb crystal does not play a relevant role in magnetar crust. As the density increases, the electron energy raises greatly as compared to the total energy, which is very advantageous for electronic capture processes. however, the lattice energy influence remain negligible. So, we ignore the influence of SMFs on the lattice energy, the EC and NELRs. On the other hand, the cyclotron energy $\hbar\omega_{ce}$ is much larger than the typical Coulomb energy, Therefore, the properties of atoms, molecules and condensed matter are qualitatively changed by the magnetic field when $B \gg 2.3505 \times 10^9\text{G}$. The usual perturbative treatment from the magnetic influence on Zeeman splitting of atomic energy levels does not apply in such regime of SMFs due to the Coulomb forces act as a perturbation to the magnetic forces(Garstang. 1977). The Coulomb force becomes much more effective in binding the electrons along the magnetic field direction due to the extreme confinement of the electrons in the transverse direction

(i.e. perpendicular to the magnetic field). The atom attains a cylindrical structure. Moreover, it is possible for these elongated atoms to form molecular chains by covalent bonding along the field direction.

One can also see that as SMFs increases, the change of NELRs will reflect some difference due to strong quantum effects in SMFs from Figures 5-6. As the density increases, when $\rho \geq \rho_B$ and $T \leq T_B$, where $\rho_B = 7.04 \times 10^3 Y_e^{-1} B_{12}^{3/2} \text{ g/cm}^3$, $T_B = 1.34 \times 10^8 B_{12} (1 + x_e^2(\nu))^{-1/2} \text{ K}$, the electrons will be strongly degenerate, and populate many Landau levels (Lai. 2001, 2015). The magnetic field is termed weakly quantizing. Thus the chemical potential, EC rates, and NELRs are only slightly affected by SMFs. With increasing T , the oscillations become weaker because of the thermal broadening of the Landau levels. When $T \geq T_B$ or $\rho \gg \rho_B$, more electrons will populate many Landau levels and the thermal widths of the Landau levels ($\sim kT$) are higher than the level spacing. The magnetic fields have almost no influence on the EC and NELRs.

GT strength distributions play an important role in EC process in the astrophysical context. Fassio-Canuto, L. (1969), and Canuto et al. (1977) demonstrated that the GT transition matrix elements for EC don't depend on the magnetic fields. Thus we will neglect the effect of SMFs on the GT properties of nuclei in this paper. A strong phase space dependence makes the EC rates more sensitive to GT distributions than to total strengths. We present GT strength distributions from shell model Monte Carlo studies of some typical fp-shell iron group nuclei in Figures 7-8. We also display the experimental data about GT distributions (Alford et al. 1993; Williams et al. 1995; El-Kateb et al. 1994; Rapaport et al. 1984), which are obtained from intermediate-energy charge exchange (n, p) or (p, n) cross sections at forward angles, which are proportional to the GT strength. We exclude contributions from other multipolarities for these experimental distributions, which extend only to 8 MeV in the daughter nucleus. We compare our SMMC results for the GT_+ distribution against experiment in Figures 7-8. One finds that the SMMC results for all even-even nuclei (e.g., $^{54,56}\text{Fe}$; $^{58,60,62}\text{Ni}$) have been smeared with Gaussians of standard deviation of 1.77 MeV to account for the finite exper-

imental resolution. From the perspective of (n, p) experiment, the GT_+ strength is significantly fragmented over many states, and these distributions centroids and widths are reproduced very well in the SMMC approach. Our results for the total strengths are agreed well with the experimental data. For example, the renormalized $B(GT_+)$ strengths from SMMC approach are 4.120, 2.682, 4.542, 3.510, 2.410 MeV for $^{54,56}\text{Fe}$, $^{58,60,62}\text{Ni}$, respectively. And the $B(GT_+)$ strengths from experiment are 3.70, 2.601, 4.203, 3.200, 2.600 MeV for the same nuclei, respectively. On the other hand, for some odd-A nuclei (e.g., ^{51}V , ^{59}Co , ^{55}Mn), SMMC results from the (n, p) direction are also in good agreement with the data of experiment (Alford et al. 1993; El-Kateb et al. 1994; Rapaport et al. 1984).

The structure and composition of the crust is important in the thermal and magnetic evolution of neutron stars. The SMFs not only strongly influence on the weak interaction rates and NELRs, but also influence the late evolution and determine the core entropy and electron to baryon ratio of magnetars. Tables 1-2 display our results of the maximum value of NELRs when $10 < B_{12} < 1000$ in different astrophysical environments. We find the maximum value of the NELRs will get to 5.694×10^7 , 7.942×10^7 , 7.760×10^7 , 6.376×10^7 , 6.444×10^7 , 6.567×10^7 , 6.701×10^7 , 6.068×10^7 when $B_{12} = 10^3$ at relatively low temperature and high density surrounding (i.e. $\rho_7 = 106$, $T_9 = 0.233$) for ^{56}Fe , $^{55,56,57,58}\text{Co}$, $^{56,57}\text{Ni}$, and ^{48}V , respectively. Nevertheless, under relativistic high temperature and high density surrounding (i.e. $\rho_7 = 106$, $T_9 = 15.53$), the maximum value of the NELRs will get to 1.062×10^8 , 1.195×10^8 when $B_{12} = 10^3$ for ^{54}Cr , and ^{47}V , respectively.

According to above discussion, we can draw a conclusion that the SMFs has a significant influence on the NELRs for a given temperature-density point. Generally the stronger the density and the lower the SMFs, the larger affect on the NELRs becomes. One can also find, when $10^{14}\text{G} \leq B \leq 10^{16}\text{G}$, for most iron group nuclei, the rates decrease greatly for a given temperature-density point. The reason is that the Fermi energy of electrons decreases, but the binding energy of the nucleus will increase with the increasing of SMFs when the temperature and density are constant. Thereby, these lead to more and more elec-

trons whose energy will be less than the threshold for EC process.

Tables 3-4 display the comparisons of our results with those of FFN (Fuller et al. 1980, 1982)(λ_{NEL}^0 (FFN)), and NKK(λ_{NEL}^0 (NKK)) (Nabi & Klapdor-Kleingothals 1999) at $\rho/\mu_e = 10^7, T_9 = 1, 3$. For the case without SMFs, at relativistic low temperature $T_9 = 1$, One finds that our rates are about close to five orders magnitude lower than FFN (e.g., for ^{60}Ni , ^{60}Co), and NKK(e.g., ^{57}Mn , $^{55,56}\text{Cr}$). However, at the relativistic high temperature $T_9 = 3$, our numerical results are in good agreement with those of NKK, but are about one order magnitude lower than those of FFN. For the case with SMFs, due to SMFs, our rates at $T_9 = 1$ can increase by more than four orders of magnitude when $B_{12} < 10^2$, and then decrease by more than three orders of magnitude as the magnetic fields increases to $B_{12} = 10^4$. On the other hand, our NELRs for some iron group nuclei can be about five orders of magnitude higher than those of FFN, NKK.

Due to the electron capture Q-value for the neutron rich nuclide (e.g., ^{60}Fe) has not been measured, FFN has to use the Seeger & Howard. (1975) Semiempirical atomic mass formula to estimate them. Thus, the Q-value used in the effective rates are quite different. For instance, For odd-A nuclei (e.g., ^{59}Fe), FFN places the centroid of the GT strength at too low excitation energies (we can reference the detailed discussed in Fuller et al. (1982, 1985)). The method for truncation of a state-density integral for calculation of the nuclear partition function from FFN's work was also criticized by Tubbs & Koonin. (1979). So their rates are somewhat overestimated. Some researches (e.g., Langanke et al. (2001); Langanke & Martinez-Pinedo. (1998)) showed that the works of FFN are an oversimplification and therefore, the accuracy can be limited due to a so-called Brinks hypothesis was adopted in their calculations. This hypothesis assumes that the GT strength distribution on excited states is the same as for the ground state, only shifted by the excitation energy of the state. This hypothesis is used by FFN due to no experimental data is available for the GT strength distributions from excited states. When FFN calculated the GT strength functions from excited states, they seemed not to employ any microscopic theory.

NKK expanded the FFN's works and analyzed

nuclear excitation energy distribution by using the pn-QRPA theory. The NKK rates are generally suppressed as compared to the rates of FFN for the case without SMFs. They had taken into consideration of the particle emission processes, which constrain the parent excitation energies. By the pn-QRPA theory, NKK calculated more stronger GT strength distribution from these excited states as compared to those assumed from Brink's hypothesis of FFN. On the other hand, A choice of particle threshold decay as the cutoff parameter for parent excitation energy seems to be a reasonable choice as also discussed earlier by Fuller et al. (1978). Thus, the parent excitation energy considered in NKK, are considerably lower as compared to those of FFN. However in the GT transitions considered process in NKK, only low angular momentum states are considered.

The method of SMMC is actually adopted to analyze the electron capture reaction by an average of GT intensity distribution. But the calculated results of NELRs for most nuclei are generally smaller than other methods, especially for some odd-A nuclides(e.g., $^{59,60}\text{Fe}$). The charge exchange reactions (p, n) and (n, p) make it possible to observe in the process of weak interaction, especial for the information of the total GT strength distribution in nuclei. The experimental information is particularly rich for some iron group nuclei and it is the availability of both GT^+ and GT^- , which makes it possible to study in detail the problem of renormalization of $\sigma\tau$ operators. We have calculated the total GT strength in a full p-f shell calculation, resulting in $B(\text{GT}) = g_A^2 |\langle \vec{\sigma}\tau_+ \rangle|^2$, where g_A^2 is axial-vector coupling constant. For example, in magnetars the electron capture on ^{59}Fe is dominated by the wave functions of the parent and daughter states. The total GT strength for ^{59}Fe in a full p-f shell calculation, is resulting in $B(\text{GT}) = 10.1g_A^2$ (Langanke et al. 2001; Langanke & Martinez-Pinedo. 1998). For instance, the total GT strength of the other important nuclide ^{56}Fe and ^{56}Ni in a full *pf*-shell calculation can be found in the Ref. (Dean et al. 1998). An average of the GT strength distribution is in fact obtained by SMMC method. A reliable replication of the GT distribution in the nucleus is carried out and detailed analysis by using an amplification of the electronic shell model. Thus the method is relative accuracy.

In summary, by analyzing the influence on NELRs of SMFs in the surface of magnetars. One can see that the SMFs has an significantly effect on NELRs for different nuclides, particularly for some heavier nuclides, whose threshold is negative at higher density. According to above calculations and discussion, one concludes that the NELRs can increase by more than four orders magnitude. As the magnetic fields increases, the NELRs decreases greatly by more than three orders magnitude. On the other hand, we compared our results in SMFs with those of FFN, and NKK. For the case without SMFs, One finds that our rates are about close to five orders magnitude lower than FFN, and NKK at relativistic low temperature $T_9 = 1$. However, at the relativistic high temperature $T_9 = 3$, our results are in good agreement with those of NKK, but about one order magnitude lower than those of FFN. For the case with SMFs, our NELRs for some iron group nuclei can be about five orders of magnitude higher than those of FFN, and NKK.

5. Conclusions and outlooks

The properties of matter in magnetars surface about SMFs has always been an interesting and challenging subject for physicists. It is obviously an important component of neutron star research for the matter in strong magnetic fields. In particular, some thermal and magnetic evolution from cooling of neutron stars require a detailed theoretical understanding of the physical properties of highly-magnetized atoms, molecules, and condensed matter. In this paper, we have focused on the electronic structure and the properties of matter in SMFs in magnetars. We have also discussed the influences of SMFs on electron Fermi energy, binding energy per nuclei, and single-particle level structure in magnetars surface based on the relativistic mean-field effective interactions theory. By using the method of SMMC, and the RPA theory, we detailed analyze the NELRs by EC process of iron group nuclei. We also compare our results in SMFs with those of FFN, and NKK, which are in the case without SMFs.

Firstly, we analyse the influence of the SMFs on NELRs when temperature and density are constant in the process of EC. We find the influence of SMFs on NELRs is very obvious and significant. At $T_9 = 0.233$, when $B_{12} < 100$, the SMFs

has a slight influence on the NELRs for most nuclides. Nevertheless, the NELRs increases by more than four orders of magnitude at $T_9 = 15.53$ when $B_{12} < 100$. And then, the NELRs rates decrease by more than three orders of magnitude when $B_{12} > 100$ at relatively high temperature (e.g., at $T_9 = 15.53$ for $^{52-61}\text{Fe}$, $^{55-60}\text{Co}$ and $^{56-63}\text{Ni}$).

Secondly, we also discuss the influence of density on NELRs at different temperature and magnetic fields point in the process of EC. One finds that the NELRs increase greatly and even exceed by four orders of magnitude for a certain value of magnetic field and temperature. With increasing of the density, there are almost not influence of density on NELRs. On the other hand, for the density around $\rho_7 = 10^2$, there is an abrupt increase in NELRs when $B_{12} \geq 10^{3.5}$. Such jumps are an indication that the underlying shell structure has changed in a fundamental way due to single-particle behavior by SMFs.

Finally, we compare our results with those of FFN, NKK due to different methods for calculating the NELRs. For the case without SMFs, one finds that our rates are about close to five orders magnitude lower than FFN, and NKK at relativistic low temperature $T_9 = 1$. However, at the relativistic high temperature $T_9 = 3$, our results are in good agreement with those of NKK, but about one order magnitude lower than those of FFN. For the case with SMFs, our NELRs for some iron group nuclei can be about five orders of magnitude higher than those of FFN, and NKK.

On the other hand, The composition, and its structure at the outer crust of magnetar is fundamentally determined by the energies of isolated nuclei, such as the binding energy, the kinetic energy of electrons and the lattice energy. We discuss the influence of SMFs on the binding energy of the nuclei, single-particle level structure, and electron Fermi energy. One finds that the NELRs increases due to increase of the electron Fermi energy, and the change of single-particle level structure by SMFs. On the contrary, the NELRs decreases due to increase of the binding energy of the nuclei by SMFs.

As we all know, the NELRs by EC play an important role in the dynamics process and cooling mechanism of magnetars. The NELRs also is a main parameter, which leads to thermal evolution and magnetic evolution of magnetars. Re-

Table 1: The maximum value of NELRs ($\lambda_{\text{NEL(max)}}^B$) at relativistic low temperature $T_9 = 0.233$ for different density when $10 \leq B_{12} \leq 1000$. Note all the NELRs is unit of $m_e c^2 s^{-1}$.

Nuclide	$\rho_7 = 5.86, T_9 = 0.233$		$\rho_7 = 14.5, T_9 = 0.233$		$\rho_7 = 50, T_9 = 0.233$		$\rho_7 = 106, T_9 = 0.233$	
	B_{12}	$\lambda_{\text{NEL(max)}}^B$	B_{12}	$\lambda_{\text{NEL(max)}}^B$	B_{12}	$\lambda_{\text{NEL(max)}}^B$	B_{12}	$\lambda_{\text{NEL(max)}}^B$
⁵² Fe	61.36	3.482e6	141.7	8.071e6	497.7	2.834e7	1.0e3	5.694e7
⁵³ Fe	61.36	3.319e6	141.7	8.070e6	497.7	2.832e7	1.0e3	5.477e7
⁵⁴ Fe	53.37	3.039e6	141.7	8.069e6	497.7	2.726e7	1.0e3	5.476e7
⁵⁵ Fe	53.37	3.037e6	141.7	7.763e6	497.7	2.725e7	1.0e3	5.694e7
⁵⁶ Fe	53.37	2.333e6	141.7	6.198e6	497.7	2.124e7	1.0e3	4.269e7
⁵⁷ Fe	53.37	2.332e6	141.7	6.196e6	432.9	1.893e7	1.0e3	4.373e7
⁵⁸ Fe	53.37	1.645e6	141.7	3.318e6	432.9	1.213e7	1.0e3	2.803e7
⁵⁹ Fe	53.37	1.642e6	141.7	3.317e6	432.9	1.335e7	1.0e3	3.083e7
⁶⁰ Fe	53.37	9.998e5	141.7	1.697e6	432.9	8.110e6	1.0e3	1.645e7
⁶¹ Fe	53.37	7.254e5	141.7	1.059e6	432.9	5.884e6	1.0e3	1.032e7
⁵⁵ Co	61.36	4.873e6	141.7	1.126e7	497.7	3.953e7	1.0e3	7.942e7
⁵⁶ Co	61.36	4.394e6	141.7	1.100e7	497.7	3.862e7	1.0e3	7.760e7
⁵⁷ Co	53.37	3.403e6	141.7	9.038e6	497.7	3.173e7	1.0e3	6.376e7
⁵⁸ Co	53.37	3.439e6	141.7	9.134e6	497.7	3.207e7	1.0e3	6.444e7
⁵⁹ Co	53.37	2.187e6	141.7	5.810e6	497.7	1.841e7	1.0e3	4.099e7
⁶⁰ Co	53.37	2.057e6	141.7	4.991e6	497.7	1.541e7	1.0e3	3.854e7
⁵⁶ Ni	53.37	4.112e6	141.7	9.309e6	497.7	3.269e7	1.0e3	6.567e7
⁵⁷ Ni	53.37	4.111e6	141.7	9.499e6	497.7	3.335e7	1.0e3	6.701e7
⁵⁸ Ni	53.37	2.596e6	141.7	6.895e6	497.7	2.421e7	1.0e3	4.865e7
⁵⁹ Ni	53.37	2.966e6	141.7	7.879e6	497.7	2.766e7	1.0e3	5.558e7
⁶⁰ Ni	53.37	2.070e6	141.7	5.498e6	497.7	1.930e7	1.0e3	3.879e7
⁶¹ Ni	53.37	1.425e6	141.7	3.785e6	497.7	1.238e7	1.0e3	2.670e7
⁶² Ni	53.37	1.004e6	141.7	2.451e6	497.7	7.552e6	1.0e3	1.847e7
⁶³ Ni	53.37	1.003e6	141.7	2.242e6	497.7	6.933e6	1.0e3	1.880e7
⁵⁵ Mn	53.37	2.564e6	141.7	6.652e6	432.9	2.080e7	1.0e3	4.805e7
⁵⁶ Mn	53.37	2.810e6	141.7	6.299e6	432.9	2.799e7	1.0e3	5.226e7
⁵⁷ Mn	53.37	2.033e6	141.7	3.826e6	432.9	1.649e7	1.0e3	3.711e7
⁵⁸ Mn	53.37	1.431e6	141.7	2.401e6	432.9	1.160e7	869.7	2.332e7
⁵⁹ Mn	53.37	9.986e5	141.7	1.392e6	432.9	8.257e6	869.7	1.659e7
⁶⁰ Mn	53.37	8.896e5	141.7	1.262e6	432.9	8.477e6	869.7	1.703e7
⁶¹ Mn	53.37	4.977e5	141.7	6.635e5	432.9	5.568e6	869.7	1.130e7
⁶² Mn	53.37	4.394e5	141.7	6.015e5	432.9	5.567e6	869.7	1.131e7
⁵³ Cr	53.37	2.384e6	123.3	5.507e6	497.7	1.785e7	1.0e3	4.467e7
⁵⁴ Cr	53.37	5.669e6	123.3	1.310e7	497.7	3.873e7	1.0e3	1.062e8
⁵⁵ Cr	53.37	1.882e6	123.3	4.349e6	497.7	9.702e6	1.0e3	3.270e7
⁵⁶ Cr	53.37	1.375e6	123.3	3.177e6	497.7	5.524e6	869.7	3.241e7
⁵⁷ Cr	53.37	1.769e6	123.3	4.425e6	497.7	6.898e6	869.7	3.122e7
⁵⁸ Cr	46.62	1.019e6	123.3	3.081e6	497.7	3.540e6	869.7	2.173e7
⁵⁹ Cr	46.62	1.038e6	123.3	2.757e6	497.7	2.801e6	869.7	1.945e7
⁶⁰ Cr	53.37	3.853e5	123.3	1.023e6	497.7	7.184e5	869.7	7.220e6
⁴⁷ V	61.36	7.333e6	141.7	1.694e7	497.7	5.948e7	1.0e3	1.195e8
⁴⁸ V	53.37	3.239e6	141.7	8.602e6	497.7	3.020e7	1.0e3	6.068e7
⁴⁹ V	53.37	2.526e6	141.7	6.709e6	497.7	2.356e7	1.0e3	4.733e7
⁵⁰ V	53.37	2.910e6	141.7	7.729e6	497.7	2.513e7	1.0e3	5.453e7
⁵⁶ V	46.62	2.268e6	141.7	6.025e6	497.7	2.115e7	869.7	4.251e7

Table 2: The maximums value of NELRs ($\lambda_{\text{NEL(max)}}^B$) at relativistic high temperature $T_9 = 15.33$ for different density condition when $10 \leq B_{12} \leq 1000$. Note all the NELRs is unit of $m_e c^2 s^{-1}$.

	$\rho_7 = 5.86, T_9 = 15.53$		$\rho_7 = 14.5, T_9 = 15.53$		$\rho_7 = 50, T_9 = 15.53$		$\rho_7 = 106, T_9 = 15.53$	
Nuclide	B_{12}	$\lambda_{\text{NEL(max)}}^B$	B_{12}	$\lambda_{\text{NEL(max)}}^B$	B_{12}	$\lambda_{\text{NEL(max)}}^B$	B_{12}	$\lambda_{\text{NEL(max)}}^B$
⁵² Fe	61.36	3.441e6	141.7	8.043e6	497.7	2.824e7	1.0e3	5.693e7
⁵³ Fe	61.36	3.185e6	141.7	7.754e6	497.7	2.713e7	1.0e3	5.477e7
⁵⁴ Fe	61.36	2.949e6	141.7	7.753e6	497.7	2.712e7	1.0e3	5.476e7
⁵⁵ Fe	53.37	3.039e6	141.7	8.029e6	497.7	2.777e7	1.0e3	5.693e7
⁵⁶ Fe	53.37	2.333e6	141.7	5.920e6	497.7	1.982e7	1.0e3	4.263e7
⁵⁷ Fe	53.37	2.278e6	141.7	5.793e6	432.9	1.893e7	1.0e3	4.348e7
⁵⁸ Fe	53.37	1.494e6	123.3	3.455e6	432.9	1.213e7	1.0e3	2.741e7
⁵⁹ Fe	53.37	1.637e6	123.3	3.801e6	432.9	1.335e7	1.0e3	2.893e7
⁶⁰ Fe	53.37	9.798e5	123.3	2.310e6	432.9	8.107e6	1.0e3	1.604e7
⁶¹ Fe	53.37	6.828e5	123.3	1.675e6	432.9	5.876e6	1.0e3	1.033e7
⁵⁵ Co	61.36	4.677e6	141.7	1.125e7	497.7	3.949e7	1.0e3	7.942e7
⁵⁶ Co	61.36	4.286e6	141.7	1.099e7	497.7	3.847e7	1.0e3	7.760e7
⁵⁷ Co	53.37	3.403e6	141.7	9.002e6	497.7	3.123e7	1.0e3	6.375e7
⁵⁸ Co	53.37	3.439e6	141.7	8.996e6	497.7	3.050e7	1.0e3	6.438e7
⁵⁹ Co	53.37	2.187e6	141.7	5.520e6	497.7	1.796e7	1.0e3	4.083e7
⁶⁰ Co	53.37	2.055e6	141.7	4.862e6	497.7	1.537e7	1.0e3	3.801e7
⁵⁶ Ni	61.36	3.984e6	141.7	9.309e6	497.7	3.268e7	1.0e3	6.567e7
⁵⁷ Ni	61.36	3.958e6	141.7	9.497e6	497.7	3.333e7	1.0e3	6.701e7
⁵⁸ Ni	61.36	2.689e6	141.7	6.890e6	497.7	2.412e7	1.0e3	4.864e7
⁵⁹ Ni	53.37	2.966e6	141.7	7.853e6	497.7	2.729e7	1.0e3	5.557e7
⁶⁰ Ni	53.37	2.070e6	141.7	5.424e6	497.7	1.844e7	1.0e3	3.876e7
⁶¹ Ni	53.37	1.425e6	141.7	3.645e6	497.7	1.204e7	1.0e3	2.663e7
⁶² Ni	53.37	9.852e5	141.7	2.367e6	432.9	7.997e6	1.0e3	1.837e7
⁶³ Ni	53.37	1.001e6	123.3	2.318e6	432.9	8.140e6	1.0e3	1.821e7
⁵⁵ Mn	53.37	2.563e6	141.7	6.261e6	432.9	2.080e7	1.0e3	4.768e7
⁵⁶ Mn	53.37	2.805e6	123.3	6.492e6	432.9	2.279e7	1.0e3	5.126e7
⁵⁷ Mn	53.37	2.016e6	123.3	4.697e6	432.9	1.649e7	1.0e3	3.484e7
⁵⁸ Mn	53.37	1.392e6	123.3	3.305e6	432.9	1.160e7	869.7	2.332e7
⁵⁹ Mn	53.37	9.343e5	123.3	2.351e6	432.9	8.239e6	869.7	1.659e7
⁶⁰ Mn	46.62	8.089e5	123.3	2.409e6	432.9	8.405e6	869.7	1.703e7
⁶¹ Mn	46.62	4.997e5	123.3	1.580e6	432.9	5.526e6	869.7	1.128e7
⁶² Mn	46.62	4.031e5	123.3	1.561e6	432.9	5.193e6	869.7	1.131e7
⁵³ Cr	53.37	2.383e6	141.7	5.685e6	432.9	1.934e7	1.0e3	4.419e7
⁵⁴ Cr	53.37	5.656e6	123.3	1.310e7	432.9	4.598e7	1.0e3	1.027e8
⁵⁵ Cr	53.37	1.858e6	123.3	4.348e6	432.9	1.527e7	1.0e3	3.121e7
⁵⁶ Cr	53.37	1.308e6	123.3	3.176e6	432.9	1.114e7	869.7	3.241e7
⁵⁷ Cr	53.37	1.691e6	123.3	4.423e6	432.9	1.548e7	869.7	3.122e7
⁵⁸ Cr	46.62	1.160e6	123.3	3.068e6	432.9	1.063e7	869.7	2.173e7
⁵⁹ Cr	46.62	1.038e6	123.3	2.716e6	432.9	9.178e6	869.7	1.944e7
⁶⁰ Cr	46.62	3.853e5	123.3	9.703e5	432.9	3.015e6	869.7	7.193e6
⁴⁷ V	61.36	6.941e6	141.7	1.694e7	497.7	5.940e7	1.0e3	1.195e8
⁴⁸ V	53.37	3.239e6	141.7	8.586e6	497.7	2.996e7	1.0e3	6.068e7
⁴⁹ V	53.37	2.526e6	141.7	6.639e6	497.7	2.267e7	1.0e3	5.433e7
⁵⁰ V	53.37	2.910e6	141.7	7.405e6	497.7	2.414e7	1.0e3	4.730e7
⁵⁶ V	46.62	2.268e6	123.3	5.994e6	432.9	2.073e7	869.7	4.249e7

Table 3: Comparisons of our calculations $\log 10(\lambda_{\text{NEL}}^B(\text{LJ}))$ in SMFs for some typical iron group nuclei with those of FFN ($\log 10(\lambda_{\text{NEL}}^0(\text{FFN}))$) (Fuller et al. 1982, 1985), NKK ($\log 10(\lambda_{\text{NEL}}^0(\text{NKK}))$) (Nabi & Klapdor-Kleingrothaus 1999), and ours ($\log 10(\lambda_{\text{NEL}}^0(\text{LJ}))$), which are for the case without SMFs at $\rho/u_e = 10^7 \text{g/cm}^3$, $T_9 = 1$. Note all the NELRs is unit of MeVs^{-1}

Nuclide	$\log 10(\lambda_{\text{NEL}}^0(\text{FFN}))$	$\log 10(\lambda_{\text{NEL}}^0(\text{NKK}))$	$\log 10(\lambda_{\text{NEL}}^0(\text{LJ}))$	$\log 10(\lambda_{\text{NEL}}^B(\text{LJ}))$			
				$B_{12} = 10$	$B_{12} = 10^2$	$B_{12} = 10^3$	$B_{12} = 10^4$
⁵² Fe	-2.266	-2.207	-2.408	5.4623	1.3769	1.9555	2.9406
⁵³ Fe	-1.533	-1.367	-1.408	5.4454	0.8495	1.4371	2.4227
⁵⁴ Fe	-9.439	-8.710	-8.807	5.4470	-3.2184	-4.5502	-3.5769
⁵⁵ Fe	-4.988	-4.222	-4.817	5.4639	-2.1618	-2.1086	-1.1235
⁵⁶ Fe	-19.733	-21.613	-21.782	5.3235	-17.8704	-19.3726	-18.3976
⁵⁷ Fe	-15.352	-15.800	-15.907	5.2719	-15.5220	-16.9372	-15.9614
⁵⁸ Fe	-32.165	-32.041	-32.197	5.0051	-30.7358	-32.0685	-31.0918
⁵⁹ Fe	-27.288	-21.174	-28.299	4.9952	-28.0682	-29.3225	-28.3450
⁶⁰ Fe	-49.560	-43.170	-50.508	4.6955	-42.1232	-43.3029	-42.3247
⁵⁵ Co	-2.466	-1.853	-1.909	5.6083	0.7675	1.3545	2.3401
⁵⁶ Co	-2.316	-2.774	-2.882	5.5983	1.1178	1.7169	2.7030
⁵⁷ Co	-4.385	-4.596	-4.656	5.5130	-0.9916	-0.4964	0.4900
⁵⁸ Co	-2.511	-4.520	-4.623	5.5124	0.2398	0.8292	1.8162
⁵⁹ Co	-11.977	-11.121	-11.856	5.2615	-7.4566	-8.8876	-7.9119
⁶⁰ Co	-7.682	-12.430	-12.823	5.1847	-2.1135	-1.8874	-0.9006
⁵⁶ Ni	-3.074	-3.060	-3.103	5.5258	0.1892	0.7522	1.7372
⁵⁷ Ni	-2.830	-1.412	-1.606	5.5346	0.8998	1.4911	2.4767
⁵⁸ Ni	-10.608	-6.577	-9.001	5.3955	-2.3616	-2.7028	-1.7202
⁵⁹ Ni	-3.935	-3.763	-3.972	5.4534	-0.2020	0.3629	1.3494
⁶⁰ Ni	-16.769	-18.503	-21.697	5.2962	-13.5209	-15.0489	-14.0742
⁵⁶ Mn	-11.289	-10.253	-11.462	5.2746	-7.850	-9.1641	-8.1873
⁵⁷ Mn	-32.154	-27.400	-32.902	5.0488	-25.0826	-26.3156	-25.3380
⁵⁸ Mn	-25.530	-33.658	-33.774	4.8537	-19.5938	-20.7505	-19.77213
⁵⁹ Mn	-44.333	-38.534	-41.612	4.6066	-37.8604	-38.9445	-37.9654
⁶⁰ Mn	-29.206	-35.262	-36.124	4.5672	-30.2670	-31.2823	-30.3024
⁵³ Cr	-18.601	-18.708	-18.899	5.2452	-16.7240	-18.1043	-17.1281
⁵⁴ Cr	-35.781	-35.287	-35.814	5.5851	1.7351	2.3534	3.3416
⁵⁵ Cr	-34.262	-30.927	-35.169	4.9785	-29.4122	-30.6225	-29.6446
⁵⁶ Cr	-53.637	-46.164	-53.944	4.7316	-44.9487	-46.0808	-45.1021
⁵⁷ Cr	-41.403	-40.338	-42.526	4.8297	-39.8564	-40.9143	-39.9349
⁵⁸ Cr	-63.730	-57.779	-64.983	4.5370	-57.6312	-58.6188	-57.6386
⁵⁹ Cr	-50.130	-50.187	-51.356	4.4363	-49.6191	-50.5398	-49.5590
⁶⁰ Cr	-73.126	-68.563	-72.963	3.8418	-68.8443	-69.7016	-68.7202
⁴⁷ V	-1.816	-1.835	-1.932	5.7858	2.1492	2.7438	3.7295
⁴⁸ V	-3.214	-3.024	-3.364	5.4915	0.7222	1.3096	2.2959
⁴⁹ V	-4.081	-3.415	-4.355	5.3836	-1.4139	-0.9871	-6.6199
⁵⁰ V	-5.011	-8.005	-8.213	5.3945	0.1058	0.6896	1.6769
⁵⁶ V	-39.223	-35.798	-39.314	5.0146	2.0691	2.7072	3.6971

Table 4: Comparisons of our calculations $\log 10(\lambda_{\text{NEL}}^B(\text{LJ}))$ in SMFs for some typical iron group nuclei with those of FFN ($\log 10(\lambda_{\text{NEL}}^0(\text{FFN}))$) (Fuller et al. 1982, 1985), NKK ($\log 10(\lambda_{\text{NEL}}^0(\text{NKK}))$) (Nabi & Klapdor-Kleingrothaus 1999), and ours ($\log 10(\lambda_{\text{NEL}}^0(\text{LJ}))$), which are for the case without SMFs at $\rho/u_e = 10^7 \text{g/cm}^3$, $T_9 = 3$. Note all the NELRs is unit of MeVs^{-1}

Nuclide	$\log 10(\lambda_{\text{NEL}}^0(\text{FFN}))$	$\log 10(\lambda_{\text{NEL}}^0(\text{NKK}))$	$\log 10(\lambda_{\text{NEL}}^0(\text{LJ}))$	$\log 10(\lambda_{\text{NEL}}^B(\text{LJ}))$			
				$B_{12} = 10$	$B_{12} = 10^2$	$B_{12} = 10^3$	$B_{12} = 10^4$
⁵² Fe	6.037	5.664	5.558	5.4623	1.3805	2.0267	3.0213
⁵³ Fe	6.019	5.598	5.578	5.4454	0.8474	1.5062	2.5010
⁵⁴ Fe	6.125	5.458	5.447	5.4470	-2.1690	-2.0135	-1.0223
⁵⁵ Fe	6.283	5.357	5.347	5.4638	-1.6645	-1.3622	-0.3697
⁵⁶ Fe	5.836	5.335	5.328	5.3221	-6.8945	-6.7286	-5.7370
⁵⁷ Fe	6.110	5.120	5.075	5.2721	-6.1343	-5.9394	-4.9475
⁵⁸ Fe	5.760	5.360	5.347	5.0054	-11.0981	-10.8756	-9.8834
⁵⁹ Fe	5.781	5.458	5.443	4.9954	-10.2236	-9.9750	-8.9825
⁶⁰ Fe	5.156	4.025	4.018	4.6959	-14.8464	-14.5730	-13.5803
⁵⁵ Co	6.498	5.903	5.779	5.6083	0.7701	1.4250	2.4198
⁵⁶ Co	6.469	5.851	5.814	5.5983	1.1081	1.7812	2.7762
⁵⁷ Co	6.313	5.669	5.556	5.5130	-0.8635	-0.3161	0.6784
⁵⁸ Co	6.377	5.717	5.696	5.5096	0.2488	0.9128	1.9080
⁵⁹ Co	6.265	5.544	5.531	5.2616	-3.5425	-3.3507	-2.3588
⁶⁰ Co	6.289	7.390	7.234	5.1848	-1.6515	-1.2634	-0.2699
⁵⁶ Ni	6.492	6.000	5.863	5.5258	0.2115	0.8364	1.8309
⁵⁷ Ni	6.453	5.826	5.786	5.5346	0.8963	1.5575	2.5523
⁵⁸ Ni	6.200	5.760	5.731	5.3955	-1.7504	-1.5301	-0.5384
⁵⁹ Ni	6.286	5.751	5.682	5.4534	-0.1654	0.4649	1.4599
⁶⁰ Ni	6.234	5.590	5.560	5.2928	-5.4792	-5.3218	-4.3303
⁵⁶ Mn	5.807	5.451	5.412	5.2748	-3.6809	-3.4505	-2.4582
⁵⁷ Mn	5.686	5.466	5.432	5.0491	-9.2471	-8.9914	-7.9989
⁵⁸ Mn	5.757	5.731	5.710	4.8540	-7.4596	-7.1784	-6.1856
⁵⁹ Mn	5.236	5.004	4.997	4.6070	-13.4381	-13.1329	-12.1398
⁶⁰ Mn	5.486	5.677	5.642	4.5676	-10.9447	-10.6164	-9.6232
⁵³ Cr	5.534	5.459	5.411	5.2455	-6.5302	-6.3236	-5.3315
⁵⁴ Cr	5.276	5.518	5.484	5.5852	1.7121	2.4189	3.4147
⁵⁵ Cr	5.120	5.504	5.499	4.9789	-10.6630	-10.3997	-9.4071
⁵⁶ Cr	5.002	4.775	4.714	4.7321	-15.7682	-15.4789	-14.4860
⁵⁷ Cr	5.287	4.468	4.456	4.8302	-14.0915	-13.7775	-12.7843
⁵⁸ Cr	4.533	4.314	4.243	4.5377	-19.9556	-19.6181	-18.6247
⁵⁹ Cr	4.859	4.257	4.158	4.4369	-17.3091	-16.9494	-15.9558
⁶⁰ Cr	3.826	3.803	3.793	3.8427	-23.6672	-23.2863	-22.2925
⁴⁷ V	5.832	5.587	5.577	5.7858	2.1371	2.8070	3.8019
⁴⁸ V	5.706	5.575	5.565	5.4915	0.7208	1.3842	2.3792
⁴⁹ V	5.543	5.496	5.423	5.3829	-1.2030	-0.7171	0.2770
⁵⁰ V	5.500	5.559	5.516	5.3947	0.1198	0.7815	1.7768
⁵⁶ V	5.356	4.173	4.063	5.0149	2.0296	2.7699	3.7664

cent studies have shown that the observations of magnetars suggest that the luminosity of persistent X-ray radiated from magnetars is likely from the radiation of thermal origin, such as heating by magnetospheric current, or by EC in the outer crust. The heat released due to EC for some iron group nuclei on magnetars surface maybe balance both surface and inner temperatures of a magnetar in different degrees. However, the considerable mechanism of the X-ray source is not clear up to now. How to influence of SMFs on soft X-ray emission, which is the possible origins of the NELRs in magnetar? How to understand the nature of the cooling from NELRs in magnetar? How to influence the NELRs in the process of EC by SMFs when the magnetic pressure decreases and the crust shrinks, the density and electron Fermi energy increase? These problem of SMFs in magnetars have always been the interesting and challenging issue. Our conclusions may be helpful to the investigation of the thermal evolution, the nucleosyntheses of heavy elements, and the numerical calculations, and simulation of the neutron stars, and magnetars.

We thank anonymous referee for carefully reading the manuscript and providing valuable comments that improved this paper substantially. This work was supported in part by the National Basic Research Program of China (973 Program) under grant 2014CB845800, the National Natural Science Foundation of China under grants 11565020, 11222328, 11333004, the Natural Science Foundation of Hainan province under grant 114012.

REFERENCES

- Alhassid, Y., Dean, D. J., Koonin, S. E., Lang, G., and Ormand, W. E., 1994, *Phys. Rev. Lett.*, 72, 613
- Alford, W. P., Brown, B. A., Burzynski, S., et al., 1993, *Phys. Rev. C.*, 48, 2818
- Ahmad, Nor. Sofiah., Yusof, Norhasliza., Kassim, Hasan. 2010, *AIP Conference Proceedings.*, 1269, 357
- Aufderheide, M. B., Brown, G. E., Kuo, T. T. S., Stout, D. B., Vogel, P., 1990, *ApJ.*, 360, 241
- Basilico, D., Arteaga, D. Peña, Roca-Maza, X., Colò, G., 2015, *Phys. Rev. C.*, 92, 035802
- Baym, G., Pethick, C., and Ann, J., 1975, *ARNPS*, 25, 27
- Beaudet, Gilles., Petrosian, Vah., Salpeter, E. E., 1967, *ApJ.*, 150, 979
- Braaten, Eric., Segel, Daniel., 1993, *Phys. Rev. D.*, 48, 1478
- Broderik, A., Prakash, M., and Lattimer, J. M., 2000, *ApJ.*, 537, 351
- Bjorken, J. D., and Drell, S. D., 1964, *Relativistic Quantum Mechanics*(McGraw-Hill, New York.
- Canuto, V., Ventura, J., 1977, *Fund. Cosmic. Phys.*, 2, 203
- Cooperstein, J., Wambach, J., 1984, *Nuclear Phys. A.*, 420, 591
- Dean, D. J., Langanke, K., Chatterjee, L., Radha, P. B., Strayer, M. R., 1998, *Phys. Rev. C.*, 58, 536
- Dai, Z. G., Lu, T., and Peng, Q. H., 1993, *A&A.*, 272, 705
- El-Kateb, S. et al., 1994, *Phys. Rev. C.*, 49, 3129.
- Esposito, S., Mangano, G.; Miele, G., Picardi, I., Pisanti, O., 2003, *NuPhB.*, 658, 217
- Fassio-Canuto, L., 1969, *Phys. Rev.*, 187, 2141
- Fowler, W. A., Engelbrecht, C. A., and Woosley, S. E., 1978, *ApJ.*, 226, 984
- Fuller, G. M., Fowler, W. A., and Newman, M. J., 1980, *ApJ.S.*, 42, 447
- Fuller, G. M., Fowler, W. A., and Newman, M. J., 1982, *ApJ.*, 252, 715
- Fuller, G. M., Fowler, W. A., and Newman, M. J., 1985, *ApJ.*, 293, 1
- Gao, Z. F., Peng, Q. H., Wang, N., Chou, C. K., Huo W. S., 2011, *ApS&S.*, 336, 427
- Gao, Z. F., Wang, N., Xu, Y., Shan, H., Li, X. D., 2015, *AN.*, 336, 866
- Gambhir, Y. K., Ring, P., and Thimet, A., 1990, *Ann. Phys. (N.Y.)*, 198, 132

- Garstang, R. H. 1977, RPPh., 40, 105
- Harding, Alice K., Lai, Dong., 2006, Phys. Rev, 58, 536
- Itoh, N., Hayashi, H., Nishikawa, A., Kohyama, Y., 1996, ApJ.S., 102, 411
- Koonin, S. E., Dean, D. J., and Langanke, K., 1997, Phys. Rep., 278, 1
- Juodagalvis, A., Langanke, K., Hix, W. R., Martinez-Pinedo, G. and Sampaio, J. M., 2010, NuPhA., 848, 454
- Johnson, C. W., Koonin, S. E., Lang, G. H., and Ormand, W. E., 1992, Phys. Rev. Lett., 69, 3157
- Johnson, M. H., & Lippmann, B. A., 1949, Phys. Rev., 76, 828
- Langanke K., Kolbe E., Dean D. J., 2001, Phys. Lett. C., 63, 032801
- Langanke K., and Martinez-Pinedo G., 1998, Phys. Lett. B., 436, 19
- Lalazissis, G. A., Konig, J., and Ring, P., 1997, Phys. Rev. C 55, 540
- Lalazissis, G. A., Niksic, T., Vretenar, D., and Ring, P., 2005, Phys. Rev. C., 71, 024312
- Landau, L. D., and Lifshitz, E. M., 1977, Quantum Mechanics, 3rd. Ed. (Pergamon Press: Oxford).
- Lai, D., & Shapiro, S. L., 1991, ApJ., 383, 745
- Lai, D., 2001, Rev. Mod. Phys., 73, 629
- Lai, D., 2015, Space. Sci. Rev., 191, 13
- Liu, J. J., 2013a, ApS&S., 343, 579
- Liu, J. J., 2013b, RAA., 13, 945
- Liu, J. J., 2013c, RAA., 13, 99
- Liu, J. J., 2013d, MNRAS., 433, 1108
- Liu, J. J., 2014, MNRAS., 438, 930
- Liu, J. J., 2015, ApS&S., 357, 93
- Liu, J. J., 2016, RAA., 16, 3, eprint arXiv:1602.05501
- Nabi, J-U., 2014, eprint arXiv:1408.4321
- Nabi, J.-U., and Klapdor-Kleingrothaus, H. V., 1999, eprint arXiv: nucl-th/9907115
- Nabi, J.-U., and Klapdor-Kleingrothaus, H. V., 2004, Atomic Data and Nuclear Data Tables, 88, 237
- Ormand, W. E., Dean, D. J., Johnson, C. W., Lang, G. H., and Koonin, S. E., 1994, Phys. Rev. C., 49, 1422
- Peña Arteaga, D., Grasso, M., Khan, E., and Ring, P., 2011, Phys. Rev. C., 84, 045806
- Peng, Q. H., and Tong, H., 2007, MNRAS., 378, 159
- Peng, Q. H., Gao, Z. F., and Wang, N., 2012, AIP Conference Proceedings., 1484, 467
- Ray, A., Chitre, S. M., Kar, K., 1984, ApJ, 285, 766
- Rapaport, J., Alarcon, R., Brown, B. A., et al., 1984, Nucl. Phys. A., 427, 332
- Shapiro, S. L., and Teukolsky, S. A., 1983, Black Holes, White Dwarfs, and Neutron Stars: The Physics of Compact Objects (Wiley, New York).
- Seeger, P. A., and Howard, W. M., 1975, NuPhA., 238, 491
- Tubbs, D. L., and Koonin, S. E., 1979, ApJ., 232, 59
- Vretenar, D., Afanasjev, A. V., Lalazissis, G. A. and Ring, P., 2005, Phys. Rep., 409, 101
- Williams, A. L., Alford, W. P., Brash, E., et al., 1995, Phys. Rev. C., 51, 1144